

## Research papers

# Palynology, palynofacies and palaeoenvironment of the Serpukhovian Tazlourt Formation (Tinghir region, southern margin of the Variscan Zone, SE Morocco)

Amine Talih<sup>a,b,\*</sup>, Daniel Țabără<sup>c</sup>, Hamid Slimani<sup>a</sup>, Ralph Thomas Becker<sup>d</sup>, Imad Tmimne<sup>a</sup>, Salma Aboutofail<sup>a</sup>, Hicham El Asmi<sup>e</sup>, Soukaina Jaydawi<sup>f</sup>

<sup>a</sup> Geo-Biodiversity and Natural Patrimony Laboratory (GEOBIO), Geophysics, Natural Patrimony and Green Chemistry" Research Center (GEOPAC), Department of Geology and Remote Sensing, Scientific Institute, Mohammed V University in Rabat, Avenue Ibn Battouta, P.B. 703, 10106 Rabat-Agdal, Morocco

<sup>b</sup> Sedimentary Petrology Laboratory, Liège University, Sart Tilman B20, Allée du Six Août 12, 4000 Liège, Belgium

<sup>c</sup> "Al. I. Cuza" University of Iași, Department of Geology, 20A Carol I Blv., 700505 Iași, Romania

<sup>d</sup> Institut für Geologie und Paläontologie, Universität Münster, Corrensstraße 24, 48149 Münster, Germany

<sup>e</sup> Laboratory of Scientific Innovation in Sustainability, Environment, Education and Health in the era of AI, Department of Biology-Geology, Graduate Normal School, Sidi Mohamed Ben Abdellah University, Fez, Morocco

<sup>f</sup> Geoscience, Water and Environment Laboratory, Department of Geology, Faculty of Sciences, Mohammed V University in Rabat, Av. Ibn Battouta, B.P. 1014 Rabat, Morocco

## ARTICLE INFO

## Keywords:

Mississippian  
Serpukhovian  
Morocco  
Sub-Meseta  
Palynostratigraphy  
Palynofacies

## ABSTRACT

The microfloristic study of limestones from the Tazlourt Formation in the Tinghir region, led to the first discovery of miospores of herbaceous and sub-arborescent lycopsids small fern and sphenopsids belonging to both non-forest mire and forest mire. The palynological assemblage also includes rare marine phytoplankton (i.e. *Lophosphaeridium* spp.). Among the continental palynomorphs, significant marker taxa, such as *Grandispora spinosa*, *Dictyotrites bireticulatus*, *Cirratiradites* cf. *C. rarus*, *Schulzospora* cf. *S. campyloptera* and *Punctatisporites gretensis* enable a confident attribution to the upper Serpukhovian stage (the *subtriquetra-ornatus* or SO miospore Zone of the Western Europe). This proves the presence of uppermost Mississippian deposits at the southern front of the Moroccan Variscan chain. The kerogen released by the analyzed samples is predominantly of continental origin, mainly composed of opaque phytoclasts with different sizes and shapes, while translucent phytoclasts and miospores are less represented. The analysis of microfacies, as well as the qualitative and quantitative parameters of the various components of the palynofacies, indicates a shallow to moderately deep neritic environment and supports the existence of a connection to the "Variscan Sea" between the Anti-Atlas domain, located on the northwestern margin of the stable Gondwana craton, and the Moroccan Hercynides, situated at the southwestern margin of the Variscides. The miospores are characterized by significant alteration in texture and color, with Spore Color Index (SCI) values ranging from 7 to 9 and advanced silicification. This is likely related to the combination of tectonic events that affected the study area during the Meso- and Post-Variscan phases.

## 1. Introduction

The Carboniferous successions of the Tinghir region, located in the Sub-Meseta zone of southern Morocco (Fig. 1), are composed of siliciclastics and carbonate rocks. Various fossil groups, such as foraminifera, algae, brachiopods, conodonts, bryozoans, crinoids, and corals, represent the palaeontological archive hosted by the latter deposits. Hindermer (1954a, 1954b) was the first to describe the Carboniferous

stratigraphy in this region, extending from the upper Tournaisian to the upper Viséan.

The sedimentological study carried out by Soualhine et al. (2003) mentions the existence of Westphalian C/D (now Moscovian) strata based on a sample with the foraminifer *Hemigordius* gr. *harltoni*? Subsequently, as part of a geological mapping project at 1:50.000 scale, Schiavo et al. (2007), Dal Piaz et al. (2007), and El Boukhari et al. (2007) subdivided the Carboniferous of this region into three formations, with

\* Corresponding author.

E-mail address: [aminetalih@gmail.com](mailto:aminetalih@gmail.com) (A. Talih).

<https://doi.org/10.1016/j.revpalbo.2025.105396>

Received 15 April 2025; Received in revised form 16 June 2025; Accepted 17 June 2025

Available online 19 June 2025

0034-6667/© 2025 Elsevier B.V. All rights reserved, including those for text and data mining, AI training, and similar technologies.

the Ait Yalla Formation at the base (upper Tournaisian–lower Visean), Tinghir Formation (upper Visean–Westphalian C/D?), and Tazlourt Formation. The latter was assigned to the lower Visean on the 1:50.000 geological map. [Graham and Sevastopulo \(2008\)](#), based on foraminifera, algae and conodonts, rejected the age suggested by [Soualhiine et al. \(2003\)](#), concluding that it falls in the upper Visean. Later, [Cózar et al. \(2020\)](#) confirmed the upper Visean age for the Tinghir Formation based on foraminifera present in certain sandy limestones, contradicting the interpretation of [Graham and Sevastopulo \(2008\)](#), who suggested a placing in the Brigantian (Cf68) rather than in the Asbian (Cf6 $\alpha$ –Cf6 $\gamma$ ) substage. Finally, [Talih et al. \(2022\)](#), based on a sedimentological and palynological study, specified with certainty the upper Tournaisian–lower Visean stage for the Ait Yalla Formation, and the upper Visean stage for the Tinghir Formation.

The Tazlourt Formation, which has not yet been precisely dated, is here studied for the first time through a sedimentological and biostratigraphic analysis. This study aims to determine this formation's age, palynofacies, and sedimentary environment.

## 2. Geological setting

Multiple geodynamic events occurred in the Anti-Atlas and the Meseta domains from the Precambrian to the Meso–Cenozoic cover ([El Hassani, 2023](#)). The studied Carboniferous section occupies a position that reflects a rather complex geological heritage. The area is located in the junction of two distinct structures of the North African craton, represented by the Precambrian terrains of the Anti-Atlas to the south and the Alpine domain of the High Atlas to the north ([Fig. 2A](#)). The oldest

units are found in the Saghro Massif, known as the Saghro and Ouarzazate groups of Neoproterozoic age (e.g. [Thomas et al., 2004](#)). During the Pan-African cycle, the complex underwent tectonic–metamorphic crustal activities responsible for the fracturing and emplacement of dolerite dykes in the basement (e.g. [Soulaïmani et al., 2018](#)). To the north, these volcano-sedimentary series were covered unconformably by a Paleozoic series during the NW-SE collision phase, manifested by granitoid magmatism in a polyphase morpho-structural opening framework with a distensive character.

The Carboniferous deposits are located in the South Meseta Fault (SMF) area at the southern margin of the Sub-Meseta Zone ([Fig. 1](#)) and represent a northwestern extension of the eastern Anti-Atlas series. Successions intermediate between the Anti-Atlas platform, and the Meseta Domain occur also further westwards, in the Skoura, Ait Tamlil and Tamlel regions (e.g. [Jenny and Le Marrec, 1980](#); [Laville, 1980](#); [Houari and Hoepffner, 2003](#); [Becker et al., 2021](#)). These locations provide an opportunity to verify the controversial relationships between the two major Moroccan Hercynian structural domains, thanks to tectonic-eustatic events evidenced by their sedimentary sequences and the overall ENE-WSW to E-W structural pattern. Locally, syn-cleavage folding, southward thrusting, and the presence of a Triassic-Liassic dolerite dyke are key components of this palaeogeographic continuum, with the latter reflecting the transtensive dynamics of the early Proto-Atlantic opening.

The study area is located SE of Timadriouine in the northwestern part of the regional Paleozoic outcrop belt, with the unconformable southern margin of the large Mesozoic area positioned along the main road to the west ([Fig. 2A](#)). The vast ENE-WSW-oriented Boumalne Syncline

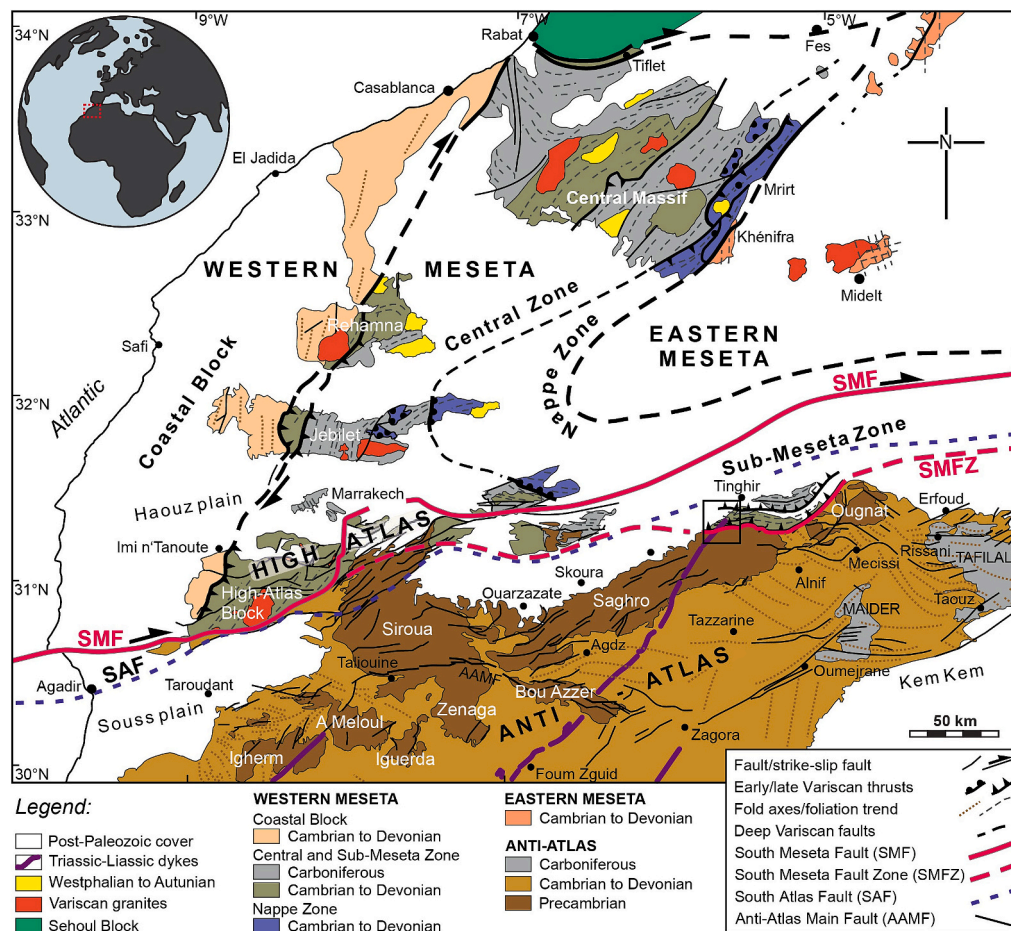


**Fig. 1.** Structural map of the Variscan Meseta Domain and the Anti-Atlas foreland in southern Morocco after [Gibb et al. \(2025\)](#), showing the location of the study area (square).

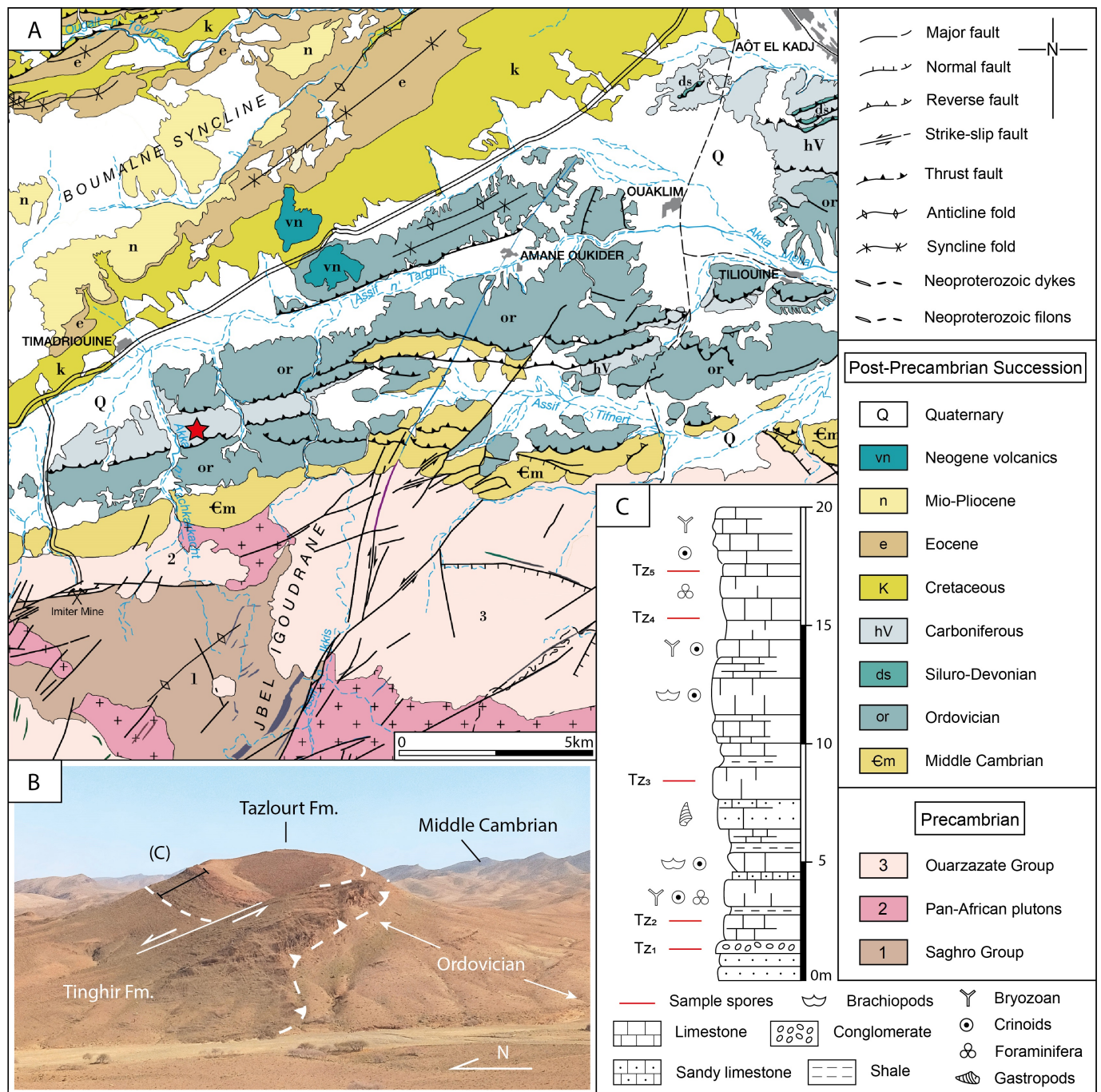


**Fig. 2.** A. Geological overview of the area southwest of Tinghir, showing the position of the Lower Carboniferous of the Tazlourt Formation (red star; re-drawn from Schiavo et al., 2007, fig. 3). B. View from the west on the study section. C. Composite lithological log of the Tazlourt Formation.

dominates the structural geology of the latter, extending from the Cretaceous to the Neogene, with its core covered by the Quaternary. The syncline is deployed as a thrust system and the result of Alpine tightening, well-marked on its northern flank, during the significant phase of Atlas shortening since the end of the Cretaceous. This structure is in contact with the Paleozoic at Fout El Kouss and a Neogene nepheline series (Neogene volcanics in Fig. 2A). The Lower Jurassic is not present locally; it overlaps the folded zone and appears exceptionally (outside Fig. 2) towards the north-western edge, highlighting the front of the High Atlas.

### 3. Material and methods

#### 3.1. Study area

The studied section (geographic coordinates 31°23'05.34" North and 5°41'37.72" West) is located near the Imiter mine, one of the oldest silver deposits in the Jbel Sagro massif (Fig. 2A). Its total thickness is 20 m (Fig. 2B–C). It is accessible by a secondary track about 2 km southeast of the village of Timadriouine. The name “Tazlourt” of this section, in the south Moroccan Amazigh language, means “sieve” in reference to its naturally narrowed shape. Located in a well-preserved sedimentary context, within a landscape shaped by a syncline, this section is of both scientific and landscape interests.



### 3.2. Sample processing and methods

Palynological data come from analyzing five samples collected from a geological section with a thickness of about 20 m (Fig. 2B–C). The rock samples were processed following standard palynological preparation techniques as described by Slimani et al. (2016). Sediment processing begins with collecting 40 g of sediment for each sample, which is crushed using a steel mortar to reduce the fragments to powder, taking care not to crush the sample too much to avoid wearing away the organic constituents. Sediment was first digested once with cold, 10% hydrochloric acid then twice for 48 h with cold, 48% hydrofluoric acid. The remaining material was boiled in 10% HCl for 20 min to remove the newly formed silicofluorides. The residues were sieved on a nylon screen with a mesh size of 15 µm, and mounted in glycerin jelly on microscope slides. Palynomorphs were observed using an Olympus BX53 transmitted light microscope. Photomicrographs (Figs. 5–6) were taken with a digital Olympus C-400 Zoom camera. Palynological slide material is housed in the botanical collection of the National Herbarium of the Scientific Institute, Mohammed V University of Rabat (Morocco).

Palynological assemblage and stratigraphic distribution of taxa, compared to those obtained from similar-aged strata in Western Europe (e.g. Clayton et al., 1977; Brindley and Spinner, 1989; McLean, 1993; Owens et al., 2004, 2005; Stephenson and Owens, 2006; Carniti and Hennissen, 2020), Morocco (Playford et al., 2008; Talih et al., 2022) North China (Feng et al., 2008), and South America (Perez Loinaze et al., 2011), enable us to determine the age of the Tazlourt Formation (for more details, see section “Biostratigraphy”).

Palynofacies analysis counted the relative abundance of unoxidized palynodebris identified in palynological slides. Three main categories of kerogen constituents proposed by Tyson (1995), Mendonça Filho et al. (2002), Aggarwal (2021), Țabără et al. (2022) have been recognized in the studied samples, namely: (i) opaque phytoclasts (OP) that showed in general equidimensional shapes and different sizes, combined with rare occurrences of lath-shaped opaque phytoclasts, both constituents representing carbonized brownish-black/oxidized to black-colored woody tissues; (ii) palynomorphs (PAL, i.e. miospores and phytoplankton taxa); and (iii) translucent phytoclasts (TP) derived from terrestrial plants.

The various palynofacies constituents have been widely used to understand the palaeodepositional environment and the transport pathway of the organic matter in shallow and deep-sea depositional settings. For example, a high proportion of equidimensional opaque phytoclasts that are small-sized and that display rounded shapes due to their transport over a prolonged period, mainly suggests a distal depositional environment (Tyson, 1993, 1995; Mendonça Filho et al., 2011; Radmacher et al., 2020). In contrast, a high amount of large, lath-shaped opaque phytoclasts represents the results of short-term transport supporting land proximity.

An additional indicator of the Carboniferous palaeoenvironment is the frequency of miospores according to their palaeobotanical and palaeoecological origins. Based on their palaeobotanical affinities, recorded taxa were assigned to three vegetation types (Jäger and McLean, 2008; Orlova et al., 2015), namely: non-forest mire (all fern-like plants and sphenopsids), forest mire (arborescent and sub-arborescent lycopsid), and colonizers. These three vegetation groups strongly depend on the depositional environment and clearly indicate a proximal–distal trend. Thus, distal sections are characterized by the predominance of miospores that belong to non-forest mire, while coastal sections are dominated by forest mire components (Jäger and McLean, 2008). Some palaeoclimatic indicators (from humid towards dry conditions) derived from the recovered miospore assemblage were interpreted according to Lindström (2003).

In order to determine the thermal maturity of organic matter, the Spore Color Index (SCI) method described by Pearson (1984), Suárez-Ruiz et al. (2012), and Hartkopf-Fröder et al. (2015) was used. This technique depends on the spore's color change, from yellow (immature stage) to brown-black (late mature/post-mature stages), with increasing

burial depths and temperature. In our investigation, the thin-walled psilate miospores were selected to determine the SCI, but this estimate should be viewed with caution due to the low number of specimens recovered.

## 4. Results

### 4.1. Sedimentary and faunal succession of the Tazlourt Formation

The Tazlourt Formation, with a local thickness of about twenty meters, is free from any overlap and partly in stratigraphic contact with the underlying Tinghir Formation (Fig. 2B–C). The transition between these two formations is gradual, with sandstones containing lumachelles of brachiopods and bivalves. The studied section begins with sandstones, alternating conglomeratic pockets with black siliceous elements, and red jasper and limestone beds (Fig. 3A). The conglomerates have a ferruginous matrix. They are composed of sub-rounded to rounded isolated lithoclasts varying in size from 1 mm to 1.5 cm. In thin-section, the main phase of this conglomerate consists of clasts of ferruginous sandstone, siltstone and quartz grains (Fig. 4A). The quartz grains are angular to sub-angular. The matrix comprises fine brownish to reddish clay with a fraction of secondary minerals, such as calcite, which often appears as microsparite and rarely as sparite.

The dark patinated limestone beds are highly recrystallized and show in thin sections an overprinted wackestone to packstone texture with a dark micritic matrix. They are characterized by a few fragments of undetermined fossils embedded in the micrite. The micrite and micro-sparite also contain silt-sized quartz grains and carbonate clasts not exceeding 1 mm in size. This limestone is affected by oxidation, which occurs as iron and manganese oxides (Fig. 4B). The dominant diagenetic phenomena are recrystallization of the micritic matrix and oxidation.

Fossil-rich sandy limestones with cross-stratification (Fig. 3B) appear above the limestone beds and show in thin-section silt-sized quartz grains packed in a ferruginous calcisiltite matrix (Fig. 4C). The grains are often sub-angular, with occasional mm-sized micritic carbonate fragments of angular to sub-angular shape. This facies shows local recrystallization of the matrix and oxidation. The fossil content includes crinoid remains, euomphalid gastropods, mollusk fragments, and undetermined brachiopods. Common euomphalids were also recorded from the middle Viséan of Skoura (Becker et al., 2021). Their taxonomy and stratigraphic distribution remain to be established.

Upwards, the limestone layers become more massive (Fig. 3D) and show at their base micro-conglomeratic pockets (Fig. 3E) as well as very characteristic black and red siliceous beds. The micro-conglomeratic facies is characterized by the presence of micritic clasts and quartz grains packed in a micritic matrix. The quartz grains do not exceed 0.5 mm and have a rounded shape, while the carbonate clasts have a sub-angular shape of about 4 mm in size. Again, there is oxidation and recrystallization.

The massive limestone shows a strongly recrystallized, micritic to microsparitic texture with irregularly developed larger sparite crystals (Fig. 4D). The facies show drying cracks filled with blackish manganese oxides. It also has a few clasts less than 1 mm in size and has an angular to sub-rounded shape. Micritic intraclasts dominate different types and were likely rearranged and re-deposited after desiccation. The facies type is affected by several secondary processes of recrystallization, cementation, and oxidation. The fossil content is quite varied, represented by bryozoans (fenestrates, rhabdomesine cryptostomes), gastropods (probably Pseudozygopleuridae), heterocorals, crinoid remains, brachiopod debris, as well as typical plates generated during subaerial exposure, which some authors (Claussen et al., 2022) have called *Palaeomicrocodium*.

### 4.2. Palynological content

The palynological assemblage recovered from five samples shows



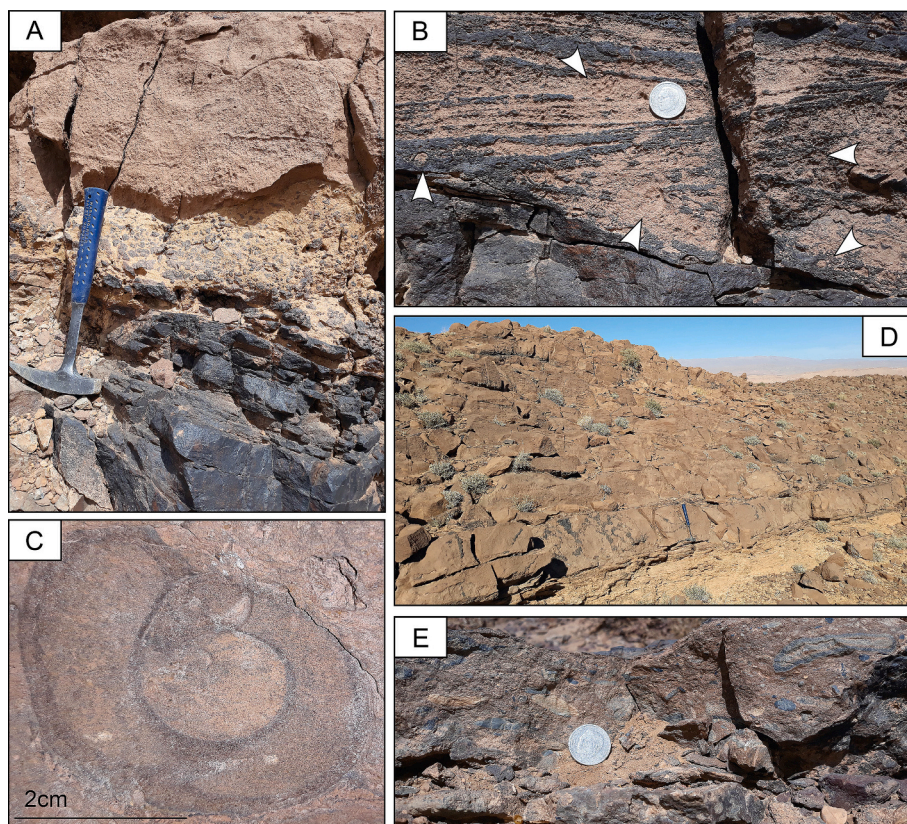


**Fig. 3.** Field photos of the Tazlourt Formation. A. Alternating sandstones, conglomerates, and limestones in the basal part of the section. B. Cross-stratified sandy limestone with varied fossil content. C. Locally very characteristic euomphalid gastropods. D. Massive limestone in the upper part of the formation. E. Micro-conglomerate with isolated, variably-sized lithoclasts in the middle part of the formation.

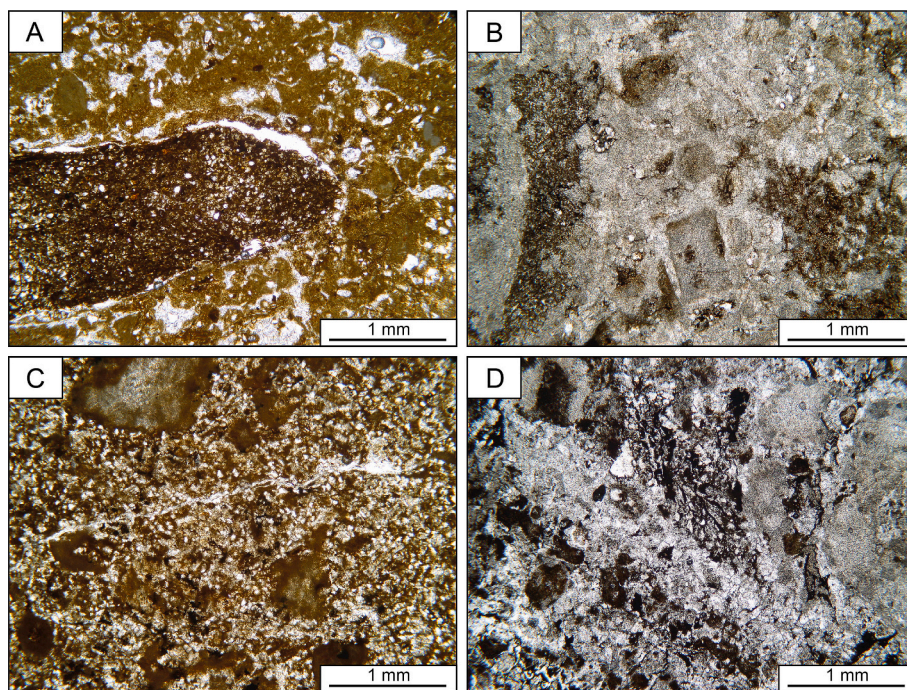


**Fig. 4.** Microfacies of the Tazlourt Formation. A. Conglomerates with isolated, rounded clast and a ferruginous matrix. B. Strongly re-crystallized and partly dolomitized limestone. C. Sandy limestone with ferruginous calcisiltite matrix. D. Strongly re-crystallized micritic to microsparitic limestone with irregularly scattered larger sparite crystals.



**Table 1**

Taxonomic list of terrestrial and marine palynomorphs identified in the Tazlourt Formation. Correlation of miospore taxa with their potential parent plants, palaeoecological groups and flora elements according to Lindström (2003), Jäger and McLean (2008), Pendleton (2012), Orlova et al. (2015), Gonzáles et al. (2016), Bek and Opluštil (2021).

Lithostratigraphic unit samples	Tazlourt Formation					Vegetation type and botanical affinity	
	Tz1	Tz2	Tz3	Tz4	Tz5	Palaeoecological groups; flora elements	Parent plants
<b>Miospores</b>							
<i>Cirratriradites</i> cf. <i>rarus</i> (Ibrahim) Schopf et al. 1944					1	Forest mire; moderately humid	Herbaceous lycopsids
<i>Densosporites</i> sp.			1	2	3	Forest mire; humid	Sub-arborescent lycopsids; <i>Sporangiostrobus</i> - <i>Bodeodendron</i>
<i>Dictyotriletes bireticulatus</i> (Ibrahim) Smith and Butterworth, 1967	3		1			Non-forest mire; moderately humid	Sphenopsids (Sphenophyllales)
<i>Dictyotriletes</i> sp.	2		1			Non-forest mire; moderately humid	Sphenopsids
<i>Grandispora spinosa</i> Hoffmeister et al. 1955				1		Non-forest mire	Fern
<i>Leiotriletes</i> sp.				1	2	Non-forest mire; neutral	Small fern
<i>Punctatisporites gretensis</i> Balme and Hennelly, 1956	1					Non-forest mire	Fern; <i>Asterotheca</i> , <i>Pecopteris</i> , <i>Scolecopteris</i>
<i>Retusotriletes</i> sp.		1		1	1	Non-forest mire	Unknown affinity
<i>Schulzospora</i> cf. <i>campyloptera</i> (Walts) Hoffmeister et al. 1955					1	Non-forest mire; neutral	Seed ferns; <i>Simpliotheca</i>
Indeterminable miospores	10	19	17	11	8		
<b>Phytoplankton</b>							
<i>Lophosphaeridium</i> spp.	1		1	1	2	Marine	

poor conservation, represented by nine miospore taxa and some specimens assigned to prasinophyte algae (Table 1). From the same section, but from an underlying sedimentary sequence assigned to the upper Visean, a relatively small number of taxa, i.e. five miospores and one phytoplankton taxon, were reported by Talih et al. (2022).

In the Tazlourt Formation, most of the identified palynomorphs represent unrecognizable miospores due to very poor preservation caused by intense weathering or high thermal alteration. For example,

the Tz2 sample contains a few palynomorphs, but almost all of them are intensely biodegraded and show an advanced thermal maturation (miospores frequently have dark brown colors; see Fig. 5), which makes it difficult to determine the taxa. However, some specimens assigned to *Cirratriradites* cf. *rarus* (Fig. 5e), *Dictyotriletes bireticulatus* (Fig. 5b, c), *Grandispora spinosa* (Fig. 5a), and *Punctatisporites gretensis* (Fig. 5l) have been recognized. A phytoplankton assemblage occurs in a few specimens throughout the entire geological section, represented only by the long-

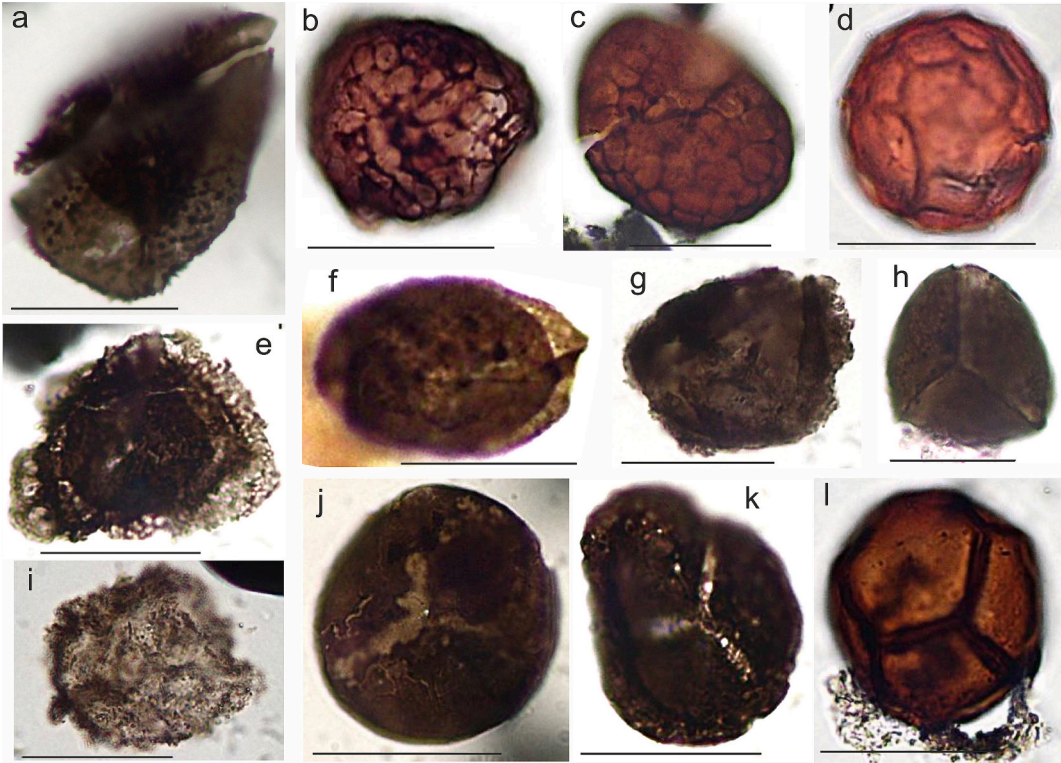


**Fig. 5.** Palynological assemblage of the Tazlourt Formation (scale bar: 40 µm). a. *Grandispora spinosa* (Tz4 sample); b-c. *Dictyotriletes bireticulatus* (b from Tz3 sample; c from Tz1 sample); d. *Dictyotriletes* sp. (Tz1 sample); e. *Cirratriradites* cf. *rarus* (Tz5 sample); f. *Schulzospora* cf. *campyloptera* (Tz5 sample); g. *Densosporites* sp. (Tz3 sample); h. *Leiotriletes* sp. (Tz4 sample); i. *Lophosphaeridium* spp. (Tz1 sample); j-k. *Retusotriletes* sp. (j from Tz2 sample; k from Tz4 sample); l. *Punctatisporites gretensis* (Tz1 sample).

ranging marine acritarch *Lophosphaeridium* spp. (Fig. 5i).

#### 4.3. Palynofacies composition

In all studied samples, the palynofacies composition is clearly dominated by opaque phytoclasts of terrestrial origin (Fig. 6), reaching 95–99% of the total particulate organic matter (POM). The equidimensional opaque phytoclasts are the most common in the Tz2–Tz5 sampling interval (Fig. 6), being generally small in size (20–40 µm), suggesting prolonged transport (up to 15 km; Tyson and Follows, 2000; Talih et al., 2022). The Tz1 sample records occurrences of large opaque phytoclasts (~200 µm; Fig. 6a) due to their short transport and shows a proximal sedimentation environment. Translucent phytoclasts and miospores represent a minor fraction, reaching maximum values of about 3–4% in the Tz1 sample at the base of the studied geological section, and lower values in the other rock samples. For the Tazlourt Formation, the SCI values of the miospores viewed under the microscope range between 7 and 9 (Fig. 5), suggesting a thermal maturity spanning the late mature stage (the end of the oil window) to the post-mature stage. A similar thermal maturity, ranging from late mature up to early post-mature stages, was previously estimated for organic matter recovered from the Aït Yalla and Tinghir formations hosted in the Jbel Asdaf section (Talih et al., 2022). This high thermal maturity of Lower Carboniferous kerogen in the Tinghir region is likely related to the combination of tectonic events that affected the study area during the Meso- and Post-Variscan phases.

## 5. Discussion

### 5.1. Biostratigraphy

A single palynological study has been performed in the Carboniferous succession of the Tinghir region, a microfloristic assemblage represented by *Rotaspora* cf. *R. knoxi* and *Vallatisporites* aff. *V. ciliaris* suggesting an upper Visean age for the Tinghir Formation (Talih et al., 2022).

The stratigraphic sequence analyzed in the present study includes about 20 m thick deposits assigned to the Tazlourt Formation, overlying the Tinghir Formation. The Tazlourt Formation yielded a palynological assemblage characterized by a restricted number of species (Table 1). However, a few species, such as *Grandispora spinosa*, *Schulzospora* cf. *campyloptera*, *Cirratiradites* cf. *rarus*, and *Dictyotrilletes bireticulatus* represent significant marker taxa for age assignment. It is based on the first occurrence (FO) and the last occurrence (LO) of the key miospore taxa, whose biostratigraphic ranges are shown in Fig. 7.

One of the biostratigraphically most important taxon identified is *Grandispora spinosa* (Fig. 5a), which is known to range from the *vetus-fracta* (VF) up to lower part of the *subtriquetra-ornatus* (SO) miospore zones (Clayton et al., 1977; Stephenson and Owens, 2006). In addition, other occurrences of this species have been reported from the upper Visean–lower Serpukhovian deposits in Scotland (Brindley and Spinner, 1989), or lower Namurian (=Serpukhovian) in Romania (Venkatachala et al., 1969). In the studied section, *Grandispora spinosa* occurs in the Tz4 sample, indicating that its age is not younger than Serpukhovian. This record is supported by *Schulzospora* cf. *campyloptera* (Fig. 7), in which LO lies at the top of the *subtriquetra-ornatus* (SO) miospore Zone (Clayton et al., 1977; Stephenson and Owens, 2006).

Two other taxa recorded in the studied samples are *Dictyotrilletes*

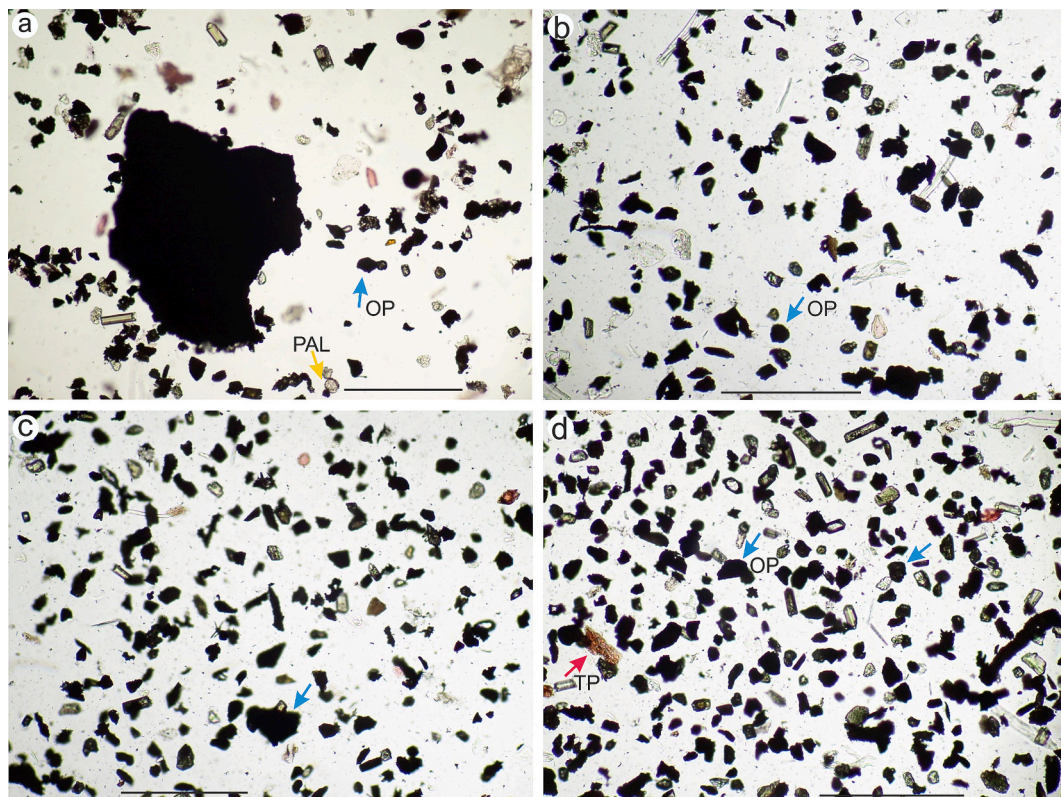


**Fig. 6.** Typical constituents of the palynodebris groups recognized in the studied samples (all unoxidized residues; scale bar: 100 µm). a. opaque phytoclasts (blue arrow), large in size, and angular forms mixed with equidimensional opaque phytoclasts, small in size, and rare palynomorphs (yellow arrow) (Tz1 sample); b-d. equidimensional opaque phytoclasts, small in size, and sometimes with rounded shapes, mixed with rare occurrences of translucent phytoclasts (red arrow) (b from Tz3 sample; c from Tz4 sample; d from Tz5 sample).



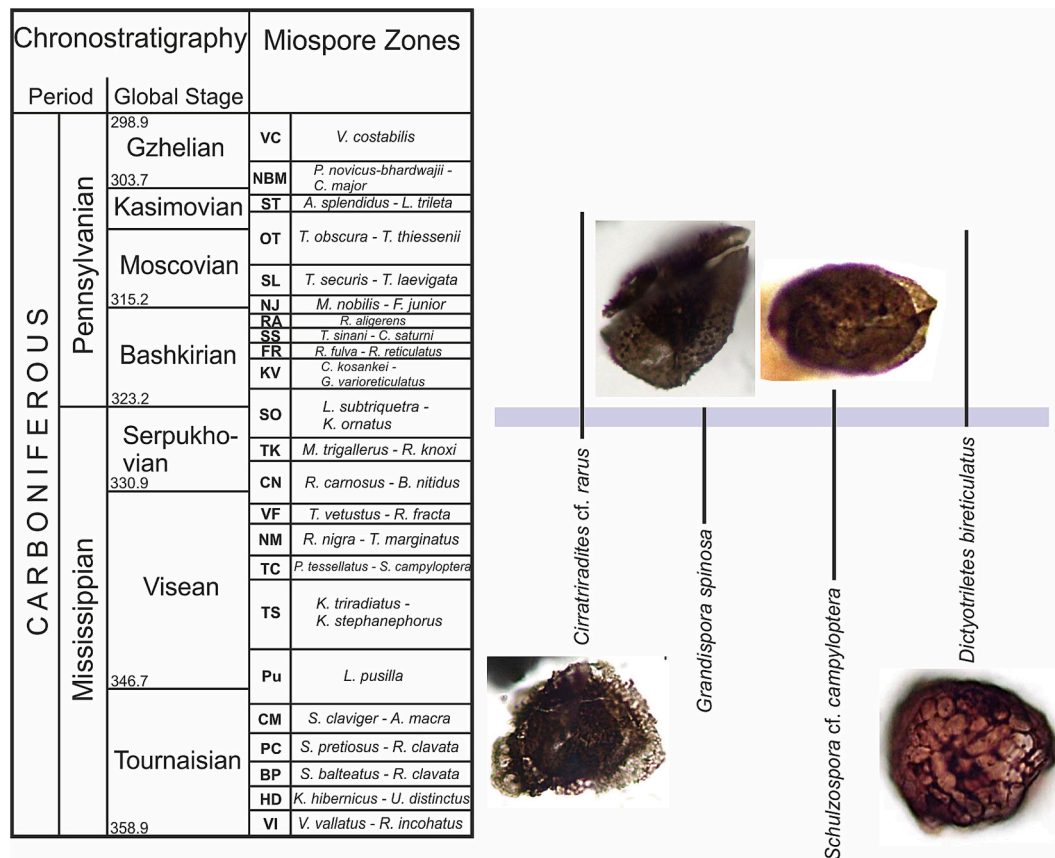


Fig. 7. General ranges of selected miospore taxa recovered from the Tazlourt Formation. The Carboniferous miospore zonation follows Clayton et al. (1977) and Owens et al. (2004).

*bireticulatus* (Fig. 5b, c) and *Cirratriadites* cf. *rarus* (Fig. 5e), having their FOs in the upper Serpukhovian (Fig. 7; Tetryuk, 1976; Clayton et al., 1977; Owens et al., 2004; Carniti and Hennissen, 2020). Both species are generally considered to indicate the Bashkirian–Moscovian range in Europe. However, in NW Africa, a good representation of both taxa may occur in an assemblage slightly older than the Bashkirian.

Sample Tz1 from the studied section displays the occurrence of *Punctatisporites gretensis* that was previously reported in the upper Serpukhovian–lower Bashkirian Subzone A of the *Raistrickia densa*–*Convolutispora muriornata* Biozone from Argentina (Perez Loinaze et al., 2011). All the bioevents listed above suggest an upper Serpukhovian age for the Tz1–Tz5 interval sampled from the Tazlourt Formation.

## 5.2. Palaeodepositional environment and palaeoclimatic significance

The previous analysis of kerogen recovered from two geological formations assigned to the upper Tournaisian–upper Visean (Ait Yalla and Tinghir formations) outcropping in the Tinghir region outlined the predominance of equidimensional opaque phytoclasts belonging to the inertinite group (Talih et al., 2022), but with a minor fraction of granular amorphous organic matter of marine origin. According to the analysis of opaque phytoclast sizes identified in these strata, the 35–42 µm size of the opaque phytoclasts corresponds to a transport distance of approximately 8 to 12.5 km from the shoreline, which was probably the uplifted Sagro-Ougnat block.

In the overlying Tazlourt Formation, the palynofacies of the Tz1 sample at the base of the section show a mixture of large-sized opaque phytoclasts (Fig. 6a) along with other small-sized phytoclasts, suggesting a shallowest environment and a shorter transport of organic particles. The organic facies of the Tz3–Tz5 sampling interval contain a fairly

similar kerogen composition, with common equidimensional opaque phytoclasts, generally having small sizes not exceeding 30 µm (Fig. 6b, c, d). This finding suggests a more distal setting for this interval. According to the method proposed by Tyson and Follows (2000) for calculating distances from the shoreline, the mean diameter of opaque phytoclasts reaching values of about 30 µm indicates a transport distance of about 15 km. Thus, a certain transgressive trend during sedimentation of the upper Serpukhovian deposits is documented by the average diameters of opaque phytoclasts.

The palynological assemblage recovered from the Tz1 sample contains several miospores belonging to non-forest mire, the parent plants of these Carboniferous taxa growing mainly as cover plants within non-flooded wetlands (DiMichele and Phillips, 2002). The Tz3–Tz5 sampling interval yielded a microflora that comes from small vegetation, such as herbaceous and sub-arborescent lycopsids, small ferns, and sphenopsids that represent both non-forest mire and forest mire, suggesting more distal sedimentation conditions. Moreover, the constant occurrence of phytoplankton proves marine conditions roughly similar to the upper Visean deposits described by Talih et al. (2022) in the neighboring Jebel Asdaf section.

The upper Serpukhovian miospore assemblage recorded in the studied section indicates moderately humid to neutral climatic conditions. An additional general aspect of the local palynology worth mentioning is the absence from all studied upper Visean–Serpukhovian deposits (see Talih et al., 2022) of *Lycospora*, the spore genus produced by several genera of arboreal lycopsids, including *Lepidodendron* and *Lepidophloios* (DiMichele et al., 2024). *Lycospora* is one of the most common Carboniferous miospore genera worldwide, and according to Bek (2012) and Tabara et al. (2021), *Lycospora*-producing plants are significant floral components of upper Mississippian–Pennsylvanian swamps and peat mires of continental interiors and coastal plains,

requiring a high-water table and relatively wet climate. It seems that such palaeoenvironment and palaeoclimate conditions were absent from the regional terrestrial source area. In summary, the upper Viséan–Serpukhovian deposits in the Tinghir region were sedimented in a middle neritic palaeoenvironment, 8–15 km from the shoreline, and under moderately humid to neutral climate conditions.

## 6. Conclusions

The study of the Upper Mississippian Tazlourt Formation in the Tinghir region, at the southern margin of the Variscan Zone (Sub-Meseta Zone), led to the following conclusions:

- 1) The mixed siliciclastic-calcareous lithofacies, with cross-bedding and conglomeratic interbeds, and the fossil content in organic matter (palynofacies components and palynomorphs) are typical for a neritic, current swept shallow to moderately deep marine environment receiving variably fine or coarse detritus from a nearby hinterland, probably from the uplifted Saghro-Ougnat Block in the south. Limestones experienced a strong diagenetic overprint.
- 2) The palynological analysis led to the first discovery of miospores derived from herbaceous and sub-arborescent lycopoids, small ferns and sphenopsids belonging to non-forest mire and forest mire. The palynological assemblage also includes rare occurrences, but constant, of marine phytoplankton, this record clearly supporting a neritic marine sedimentation. Among continental palynomorphs, significant marker miospores enable a confident attribution to the upper Serpukhovian stage.
- 3) The kerogen is predominantly of continental origin, mainly composed of opaque phytoclasts with different sizes and shapes, while translucent phytoclasts and miospores are less represented. Phytoclasts and the miospore assemblage recorded in the studied section generally indicate deposition in a middle neritic palaeoenvironment, 8–15 km from the shoreline, and moderately humid to neutral climatic conditions.
- 4) The combined lithofacies, biofacies and palynological analyses support the existence of an upper Mississippian marine connection from the Anti-Atlas domain through the Sub-Meseta to the “Variscan Sea” (Western Meseta, Moroccan Hercynides) on the northwestern margin of the stable Gondwana craton. This is supported by palaeobiogeographic marker genera, e.g., the top-Viséan/lower Serpukhovian goniatite *Ferganoceras*, which ranged from the eastern Tafilalt to the Eastern Meseta (Jerada Basin), and beyond to southern Europe (Montagne Noire).
- 5) The miospores are characterized by significant alteration in texture and color, with SCI values ranging from 7 to 9 and advanced silicification. The limestone recrystallization is likely related to the combination of tectonic events that affected the study area during the Meso- and Post-Variscan phases.

## Declaration of competing interest

The authors declare that they have no known competing financial interests or personal relationships that could have appeared to influence the work reported in this paper.

## Acknowledgements

The authors express their sincere gratitude to the editor-in-chief of the journal, Henk Brinkhuis, as well as to the reviewers, Paulo Fernandes and an anonymous, for their valuable corrections, suggestions, and comments, which significantly improved the original manuscript. Acknowledgments are also extended to the Laboratory of Palynology, Department of Geology and Remote Sensing (Scientific Institute, Mohammed University in Rabat, Morocco) for the technical support. Ahmed El Hassani (Hassan II Academy of Science and Technology,

Morocco), Andrej Ernst (Institut für Geologie, Universität Hamburg, Germany), Pedro Cózar (Instituto de Geociencias, Ciudad Universitaria, Spain), and Anne-Christine Da Silva (University of Liège, Belgium) are gratefully acknowledged for their insightful scientific discussions.

## Data availability

The authors confirm that all data necessary for supporting the scientific findings of this paper have been provided.

## References

- Aggarwal, N., 2021. Sedimentary organic matter as a proficient tool for the palaeoenvironmental and palaeodepositional settings on Gondwana coal deposits. *J. Petrol. Explor. Prod. Technol.* 12, 1–22. <https://doi.org/10.1007/s13202-021-01331-x>.
- Becker, R.T., Aboussalam, Z.S., El Hassani, A., Baidder, L., Hüneke, H., Mayer, O., Cózar, P., Helling, S., Seyffert, K., May, A., 2021. Devonian and the Carboniferous transgression in the Skoura region, Sub-Meseta Zone, Morocco. *Front. Sci. Eng. Earth Water Oceans Environ. Sci.* 10 (2), 251–333.
- Bek, J., 2012. A review of the genus *Lycospora*. *Rev. Palaeobot. Palynol.* 174, 122–135. <https://doi.org/10.1016/j.revpalbo.2011.12.008>.
- Bek, J., Oplustil, S., 2021. Early Pennsylvanian to early Permian (Bashkirian–Asselian) miospore and pollen assemblages of the Czech part of the Intra-Sudetic Basin. *Bull. Geosci.* 96 (3), 341–379. <https://doi.org/10.3140/bull.geosci.1790>.
- Brindley, S., Spinner, E., 1989. Palynological assemblages from Lower Carboniferous deposits, Burntisland district, Fife, Scotland. *Proc. Yorks. Geol. Soc.* 47 (3), 215–231. <https://doi.org/10.1144/pygs.47.3.215>.
- Carniti, A., Hennissen, J.A.L., 2020. Taxonomy Online 3: the ‘Bernard Owens Collection’ of single grain mount palynological slides: Carboniferous pollen and spores, part II. In: *British Geological Survey Open Report, OR/21/038*, 71 pp.
- Claussen, A.L., Munneke, A., Ernst, A., 2022. Bryozoan-rich stromatolites (bryostromatolites) from the Silurian of Gotland and their relation to climate-related perturbations of the global carbon cycle. *Sedimentology* 69, 162–198. <https://doi.org/10.1111/sed.12863>.
- Clayton, G., Coquel, R., Doubinger, J., Gueinn, K.J., Loboziak, S., Owens, B., Streel, M., 1977. Carboniferous miospores of Western Europe: illustration and zonation. *Med. Rijks Geol. Dienst.* 29, 1–71.
- Cózar, P., Vachard, D., Izart, A., Said, I., Somerville, I., Rodríguez, S., Coronado, I., El Houicha, M., Ouahache, D., 2020. Lower-middle Viséan transgressive carbonates in Morocco: palaeobiogeographic insights. *J. African Earth Sci.* 168, 103850. <https://doi.org/10.1016/j.jafrearsci.2020.103850>.
- Dal Piaz, G.V., Malusà, M., Eddebbi, A., El Boukhari, A., Ellero, A., Laftouhi, N., Massironi, M., Ouanaimi, H., Pertusati, P.C., Polino, R., Schiavo, A., Taj-Eddine, K., Visonà, D., 2007. Carte Géologique du Maroc au 1/50,000, feuille Taghazout-notice explicative. In: *Notes et Mémoires du Service Géologique du Maroc*, 519 (bis).
- DiMichele, W.A., Phillips, T.L., 2002. The ecology of Paleozoic ferns. *Rev. Palaeobot. Palynol.* 119, 143–159. [https://doi.org/10.1016/S0034-6667\(01\)00134-8](https://doi.org/10.1016/S0034-6667(01)00134-8).
- DiMichele, W.A., Lucas, S.G., Eble, C.F., Kerp, H., Reynolds, S.J., May, P., Pigg, K.B., 2024. A detailed stratigraphic and taphonomic reassessment of the late Paleozoic fossil flora from Promontory Butte, Arizona. *Rev. Palaeobot. Palynol.* 320, 105004. <https://doi.org/10.1016/j.revpalbo.2023.105004>.
- El Boukhari, A., Ottria, G., Algouti, A.B., Cerrina Feroni, A., Dal Piaz, G.V., Ellero, A., Ghiselli, F., Malusà, M., Massironi, M., Musumeci, G., Ouanaimi, H., Pertusati, P., Schiavo, A., Taj-Eddine, K., 2007. Carte Géologique du Maroc au 1/50,000, feuille Taroucht. Notice explicative. In: *Notes et Mémoires du Service Géologique du Maroc*, p. 520.
- El Hassani, A., 2023. A Geologist’s Paradise. Tracing Morocco’s Geological History from Early Explorers to the Modern Era. Hassan II Academy Press, Rabat, 382 pp.
- Feng, L., Huaicheng, Z., Shu, O., 2008. Late Carboniferous–Early Permian palynology of Baode (Pao-te-chou) in Shanxi Province, North China. *Geol. J.* 43, 487–510. <https://doi.org/10.1002/gj.1121>.
- Gibb, M.A., Hüneke, H., Pingel, N., Gibb, L.M., Rihter, C., Mayer, O., Aboussalam, Z.S., Becker, R.T., El Hassani, A., Baidder, L., 2025. Early Devonian bioclastic contourites in the High Atlas: a plastered drift recording the convergence between Gondwana and Laurussia (Sub-Meseta Zone, Morocco). *Geol. Soc. Lond. Spec. Publ.* 553. <https://doi.org/10.1144/SP553-2023-80>.
- González, F., Moreno, C., Lorenzo, E., Márquez, G., 2016. Factors controlling the vegetation distribution and coal-forming environments in a strike-slip basin. The Pennsylvanian Penarroya-Belmez-Espiel Basin, southern Spain. *Terra Nova* 28, 171–180. <https://doi.org/10.1111/ter.12205>.
- Graham, J.R., Sevastopulo, G.D., 2008. Mississippian Platform and Basin Successions from the Todra Valley (northeastern Anti-Atlas), southern Morocco. *Geol. J.* 43, 1–22. <https://doi.org/10.1002/gj.1095>.
- Hartkopf-Fröder, C., Königshof, P., Littke, R., Schwarzbauer, J., 2015. Optical thermal maturity parameters and organic geochemical alteration at low grade diagenesis to anchimetamorphism: a review. *Int. J. Coal Geol.* 150, 74–119. <https://doi.org/10.1016/j.coal.2015.06.005>.
- Hindermeyer, J., 1954a. Découverte de graptolites dendroïdes dans le dinantien de la région de Tinghir (flanc Nord du Sarhro-Ougnat). *C. R. Hebd. Seances Acad. Sci.* 239, 1397–1399.

- Hindermeyer, J., 1954b. Découverte du Tournaisien et tectonique prémonitoire hercynienne dans la région de Tinghir (flanc Nord du Sarhro-Ougnat). *C. R. Hebd. Seances Acad. Sci.* 239, 1824–1826.
- Houari, M.R., Hoepffner, C., 2003. Late Carboniferous dextral wrench-dominated transpression along the North African craton margin (Eastern High-Atlas, Morocco). *J. Afr. Earth Sci.* 37 (1–2), 11–24. [https://doi.org/10.1016/S0899-5362\(03\)00085-X](https://doi.org/10.1016/S0899-5362(03)00085-X).
- Jäger, H., McLean, D., 2008. Palynofacies and spore assemblage variations of upper Viséan (Mississippian) strata across the southern North Sea. *Rev. Palaeobot. Palynol.* 148, 136–153. <https://doi.org/10.1016/j.revpalbo.2007.04.005>.
- Jenny, J., Le Marrec, A., 1980. Mise en évidence d'une nappe à la limite meridionale du domaine hercynien dans la boutonniere d'Ait-Tamlil (Haut Atlas central, Maroc). *Eclogae Geol. Helv.* 73, 681–696.
- Laville, E., 1980. Tectonique et microtectonique d'une partie du versant sud du Haut Atlas marocain (boutonnière de Skoura nappe de Toundout). *Notes et Mémoire du Service géologique du Maroc* 41 (285), 81–184.
- Lindström, S., 2003. Carboniferous palynology of the Loppa High, Barents Sea, Norway. *Nor. J. Geol.* 83, 333–349.
- McLean, D., 1993. A Palynostratigraphic Classification of the Westphalian of the Southern North Sea Carboniferous Basin. Unpublished PhD thesis, University of Sheffield, 251 pp.
- Mendonça Filho, J.G., Carvalho, M.A., Menezes, T.R., 2002. Palinofácies. In: Dutra, T.L. (Ed.), *Técnicas e Procedimentos para o Trabalho com Fósseis e Formas Modernas Comparativas*. Unisinos, São Leopoldo, pp. 20–24.
- Mendonça Filho, J.G., Menezes, T.R., Mendonça, J.O., 2011. Organic composition (palynofacies analysis) (Chapter 5). In: ICCP Training Course on Dispersed Organic Matter, pp. 33–81.
- Orlova, O.A., Mamontov, D.A., Snigirevsky, S.M., 2015. Late Viséan (Mississippian) vegetation of the north-western part of Russia according to palaeobotanical and palynological data. *Hist. Biol.* 27 (3–4), 325–344. <https://doi.org/10.1080/08912963.2014.899117>.
- Owens, B., McLean, D., Bodman, D., 2004. A revised palynozonation of British Namurian deposits and comparisons with eastern Europe. *Micropaleontology* 50 (1), 89–103. <https://doi.org/10.2113/50.1.89>.
- Owens, B., McLean, D., Simpson, K.R.M., Shell, P.M.J., Robinson, R., 2005. Reappraisal of the Mississippian palynostratigraphy of the East Fife Coast, Scotland, United Kingdom. *Palynology* 29, 23–47. <https://doi.org/10.1080/01916122.2005.9989603>.
- Pearson, D.L., 1984. Pollen/spore color “standard”. *Phillips Petroleum Company Exploration Projects Section* (reproduced in Traverse, A., 1988). In: *Palaeopalynology*, Plate 1. Unwin, Hyman.
- Pendleton, J.L., 2012. Palynological and Palaeobotanical Investigation of the Carboniferous Deposits of the Bristol Coalfield, U.K.; Biostratigraphy, Systematics and Palaeoecology. Ph.D. Thesis. Department of Animal and Plant Sciences, University of Sheffield, 482 pp.
- Perez Loinaze, V.S., Limarino, C.O., Césari, S.N., 2011. Palynological study of the Carboniferous sequence at Rio Francia Creek, Paganzo Basin, Argentina. *Ameghiniana* 48 (4), 589–604.
- Playford, G., Gonzáles, F., Moreno, C., Al Ansari, A., 2008. Palynostratigraphy of the Sarhle Series (Mississippian), Jebilet Massif, Morocco. *Micropaleontology* 54 (2), 89–124. <https://doi.org/10.47894/mpal.54.2.01>.
- Radmacher, W., Kobos, K., Tyszyka, J., Jarzynka, A., Arz, J.A., 2020. Palynological indicators of palaeoenvironmental perturbations in the Basque-Cantabrian Basin during the latest Cretaceous (Zumaia, northern Spain). *Mar. Pet. Geol.* 112, 104107. <https://doi.org/10.1016/j.marpetgeo.2019.104107>.
- Schiavo, A., Taj-Eddine, K., Algouti, A., Benvenuti, M., Dal Piaz, G.V., Eddebbe, A., El Boukhari, A., Laftouhi, N., Massironi, M., Moratti, G., Ouanaïmi, H., Pasquare, G., Visona, D., 2007. Carte Géologique du Maroc au 1/50,000, feuille Imtir. *Notes et Mémoire du Service géologique du Maroc* 518.
- Slimani, H., Guédé, K.E., Williams, G.L., Asebriy, L., Ahmamou, M., 2016. Campanian to Eocene dinoflagellate cyst biostratigraphy from the Tahar and Sekada sections at Arba Ayacha, western External Rif, Morocco. *Rev. Palaeobot. Palynol.* 228, 26–46. <https://doi.org/10.1016/j.revpalbo.2016.01.003>.
- Soualhine, S., De Leon, J.T., Hoepffner, C., 2003. Les faciès sédimentaires carbonifères de Tisdafine (Anti-Atlas oriental): Remplissage deltaïque d'un bassin en «pull-apart» sur la bordure méridionale de l'Accident sud-atlasique. *Bulletin de l'Institut Scientifique*, Rabat 25, 31–41.
- Soulaimani, A., Ouanaïmi, H., Saddiqi, O., Baïdier, L., Michard, A., 2018. The anti-atlas pan-African belt (Morocco): overview and pending questions. *C. R. Geosci.* 350, 279–288. <https://doi.org/10.1016/j.crte.2018.07.002>.
- Stephenson, M.N., Owens, B., 2006. Taxonomy Online 2: The 'Bernard Owens Collection' of single grain mount palynological slides: Carboniferous spores part I. In: *British Geological Survey Research Report*, RR/06/05, 80 pp.
- Suárez-Ruiz, I., Flores, D., Mendonça Filho, J.G., Hackley, P.C., 2012. Review and update of the applications of organic petrology: part 1, geological applications. *Int. J. Coal Geol.* 99, 54–112. <https://doi.org/10.1016/j.coal.2012.02.004>.
- Țabără, D., Tudor, E., Chelariu, C., Olaru-Florea, R.F., 2021. Paleoenvironmental interpretation and palynoflora of Devonian - carboniferous subsurface sections from the eastern part of the Moesian Platform (Romania). *Rev. Palaeobot. Palynol.* 284, 104338. <https://doi.org/10.1016/j.revpalbo.2020.104338>.
- Țabără, D., Vasile, S., Csiki-Sava, Z., Bălc, R., Vremir, M., Chelariu, M., 2022. Palynological and organic geochemical analyses of the Upper Cretaceous Bozeș Formation at Petrești (southwestern Transylvanian Basin) - biostratigraphic and palaeoenvironmental implications. *Cretac. Res.* 134, 105148. <https://doi.org/10.1016/j.cretres.2022.105148>.
- Talih, A., Țabără, D., Slimani, H., Saadi, M., Benmlih, A., Aboutofail, S., 2022. Integrated palynology and sedimentology of the Mississippian of the Tisdafine Basin (Eastern Anti-Atlas, Morocco). *Swiss J. Palaeontol.* 141, 1–14. <https://doi.org/10.1186/s13358-022-00256-0>.
- Teteryuk, V.K., 1976. Namurian Stage analogues in the Carboniferous Period of the Donets Basin, (based on palynological data). *Geol. Zh.* 36 (1), 110–122 (in Russian).
- Thomas, R.J., Fekkak, A., Ennih, N., Errami, E., Loughlin, E.S., Gresse, P.G., Chevallier, L. P., Liégeois, J.P., 2004. A new lithostratigraphic framework for the Anti-Atlas Orogen, Morocco. *J. African Earth Sci.* 39, 217–226. <https://doi.org/10.1016/j.jafrearsci.2004.07.046>.
- Tyson, R.V., 1993. Palynofacies analysis. In: Jenkins, D.J. (Ed.), *Applied Micropalaeontology*. Kluwer Academic Publishers, Dordrecht, pp. 153–191.
- Tyson, R.V., 1995. *Sedimentary Organic Matter: Organic Facies and Palynofacies*. Chapman and Hall, London, 615 pp.
- Tyson, R.V., Follows, B., 2000. Palynofacies prediction of distance from sediment source: a case study from the Upper Cretaceous of the Pyrenees. *Geology* 28 (6), 569–571. [https://doi.org/10.1130/0091-7613\(2000\)28<569:PPPDFS>2.0.CO;2](https://doi.org/10.1130/0091-7613(2000)28<569:PPPDFS>2.0.CO;2).
- Venkatachala, B.S., Beju, D., Kar, R., 1969. Carboniferous spores and pollen from the Călăreți zone of the Moesian Platform, Romania. *Paleobotanist* 17 (1), 68–79.